Bandwidth Widening of Piezoelectric Cantilever Beam Arrays by Mass-Tip Tuning for Low-Frequency Vibration Energy Harvesting

Eduard Dechant [1], Feodor Fedulov [2], Leonid Y. Fetisov [2] and Mikhail Shamonin [1,*] 🆔

[1] East Bavarian Centre for Intelligent Materials (EBACIM),
    Ostbayerische Technische Hochschule (OTH) Regensburg, D-93053 Regensburg, Germany;
    dechant.e@live.de
[2] Research and Education Center "Magnetoelectric Materials and Devices",
    Moscow Technological University (MIREA), 119454 Moscow, Russia; ostsilograf@yandex.ru (F.F.);
    fetisovl@yandex.ru (L.Y.F.)
*   Correspondence: mikhail.chamonine@oth-regensburg.de; Tel.: +49-941-943-1105

Featured Application: The results of the present work can be used to develop vibration energy harvesters supplying wireless sensor nodes. This is feasible since the order of magnitude of harvested electrical power is 1 mW.

Abstract: Wireless sensor networks usually rely on internal permanent or rechargeable batteries as a power supply, causing high maintenance efforts. An alternative solution is to supply the entire system by harvesting the ambient energy, for example, by transducing ambient vibrations into electric energy by virtue of the piezoelectric effect. The purpose of this paper is to present a simple engineering approach for the bandwidth optimization of vibration energy harvesting systems comprising multiple piezoelectric cantilevers (PECs). The frequency tuning of a particular cantilever is achieved by changing the tip mass. It is shown that the bandwidth enhancement by mass tuning is limited and requires several PECs with close resonance frequencies. At a fixed frequency detuning between subsequent PECs, the achievable bandwidth shows a saturation behavior as a function of the number of cantilevers used. Since the resonance frequency of each PEC is different, the output voltages at a particular excitation frequency have different amplitudes and phases. A simple power-transfer circuit where several PECs with an individual full wave bridge rectifier are connected in parallel allows one to extract the electrical power close to the theoretical maximum excluding the diode losses. The experiments performed on two- and three-PEC arrays show reasonable agreement with simulations and demonstrate that this power-transfer circuit additionally influences the frequency dependence of the harvested electrical power.

Keywords: vibration energy harvesting; piezoelectric cantilever; array; bandwidth; optimization

1. Introduction

Because of the continuing improvements with respect to the power consumption of electronic integrated circuits, harvesting of the ambient energy is gaining importance for electronic devices such as wireless sensor networks [1]. Ambient mechanical vibrations represent promising sources of energy. In the majority of the practical cases, the energy from mechanical vibrations in the environment is distributed over a wide spectrum. Most of the previous works use resonant circuits, where the maximum performance can be achieved when the external frequency is close to the resonant frequency of the circuit. A piezoelectric (PE) cantilever beam is an example of such a circuit, where the

piezoelectric effect is utilized for converting mechanical energy into electric energy. Operation close to the mechanical resonance is required in order to achieve large amplitudes of mechanical deformation. The favorability of the PE transduction mechanism in applications can be explained by the larger energy density in comparison to other available effects [2–4]. To be electromechanically effective, the PE resonant circuit must possess a high quality factor Q, because the oscillation amplitude at resonance grows with the increasing parameter Q. Unfortunately, this entails a narrow-band frequency behavior of a single circuit. Tang et al. [5] and Twiefel et al. [6] published comprehensive reviews on the available technologies and recent advances in broadband vibration-based energy harvesting.

An obvious solution for increasing the bandwidth is to employ several piezoelectric cantilevers (PECs), whose mechanical resonance frequencies are distributed over the desired band in such a way that at any particular frequency at least one circuit operates close to its resonance frequency. The most general approach for designing an optimized mechanical band-pass filter has been provided by Shahruz [7,8], who developed a mathematical model where the eigenfrequency of a single beam is adjusted both by the proof mass and the beam stiffness, leading to the required dimensions of the beam. Xue et al. [9] included the PE properties of the beam elements and the electrical circuitry into the calculations. It was shown that the frequency behavior of the entire system can be influenced by connecting the PE bimorphs either in series or parallel. Ferrari et al. combined three commercially available PE bimorph cantilevers into a single array, improving the effectiveness of the overall energy conversion across a wideband frequency spectrum over the case of a single converter [10]. The tuning of resonant frequency was achieved by varying the tip mass. A broadband PE energy harvester for low-frequency ($\approx$30–47 Hz) vibrations was developed by Liu et al. [11] for micro-electro-mechanical system (MEMS) applications. Their device consisted of several beams with different stiffness and the same tip mass. In the following we refer to the mechanical vibrations as low-frequency oscillations if their frequency is below 60 Hz. Al-Ashtary et al. proposed to detune the eigenfrequency of individual standard PE bimorphs by means of magnetic force acting on the small magnet positioned at the beam tips [12]. By changing the magnetic force, the effective stiffness of the beam can be controlled. Wen et al. [13] investigated an arrays of identical MEMS-based lead zirconate titanate (PZT) PEC beams and showed that the series connection of PECs allowed for an improvement of the power output because the small (below 1 V) voltages of individual PECs were added together and the losses in a rectifier circuit could be significantly reduced. This finding has been confirmed by Zhao et al. [14] with an array of MEMS-based aluminum nitride (AlN) PECs.

Very recently, Wu et al. [15] investigated mixed (parallel/series) connection of PE oscillators and showed that the bandwidth of the array capable of switching connection patterns can be significantly enhanced in comparison to a conventional single (parallel or series) array configuration. The authors of [15] also provide a comprehensive overview of research on PE oscillator arrays. Although the general analytical solution to the problem of calculating multi-frequency responses of multiple electromechanical piezoelectric bimorph beams loaded by variable load resistance was presented five years ago [16], the more specific questions of optimization of particular PEC arrays taking into account the power-transfer circuitry have not been completely solved yet. In particular, Lien and Shu [17] used the idea of equivalent impedance to investigate the electrical response of an array of piezoelectric oscillators using distinct energy harvesting circuits. Three interface electronics systems were considered, including standard AC/DC (single full wave rectifier) and parallel/series-synchronized switch harvesting on inductor (SSHI) circuits. Lin et al. [18] investigated the electrical response of a series connection of PE vibration energy harvesters attached to various interface electronics, including standard and parallel-/series-SSHI circuits. They showed that the parallel-SSHI array system exhibits higher power output with moderate bandwidth improvement, while the series-SSHI system gives a pronounced widening of the bandwidth at the cost of peak harvested power. The standard array system with a full wave bridge rectifier shows a capability of power harvesting between these two SSHI systems.

Frequency tuning of a PEC can be done either by changing the effective mass of the beam or its stiffness. This can be achieved by variation of the cantilever geometry or material properties. In practical applications, commercially available PECs are likely to be resorted to. Such PECs are normally available in predefined steps of beam stiffness. Therefore, tuning by the tip mass is often advantageous and desirable. Hitherto, most of the papers dealing with parallel or series connections of PECs have used the same realization of the transducer (implying the same amplitude and phase of output voltages). For the mass-tip tuning, this is not the case, and this feature leads to the different behavior of the previously studied circuits, in particular parallel and series connections.

In this paper, we address the limits of tip-mass tuning and the analysis of its optimization. In the following considerations, each PEC will be supplied by an individual full wave bridge rectifier circuit. By doing so, we largely avoid the interference between different oscillators due to the different phases of output voltages. Such an idea was proposed earlier by Lien and Shu [19], who obtained analytic estimates on harvested power for various interface circuits, including the standard interface and parallel-/series-SSHI circuits. In the present paper, it will be shown that the power output depends both on the load and the resonance frequency detuning between individual PECs. The considered power-transfer circuits (denoted as standard interfaces in [19]) are simple for practical implementation. It will be also demonstrated that with such power-transfer circuit, the output power is quite close to the theoretically achievable maximum power. However, the modeling approach can be easily extended to other power transfer circuits where the consequences are known, as shown in previous publications [18]. In particular, Lien and Shu have pointed out that implementation of control circuits for SSHI techniques in addition to respective electrical rectification can be a challenging task [19].

2. Materials and Methods

As explained in [12], the majority of published works on vibration energy harvesting using multiple PEC beams are difficult to transfer to industrial applications. An engineer wishing to design a broadband vibration harvester for a particular application usually has to rely on commercially available PEC beams, which are not available off the shelf with any geometry, and on simple circuit simulation software for predicting the performance of the entire electric circuit. During the design stage of a PE energy harvester, it is important to establish a particular analytical or numerical model to estimate the output power of the system [20]. A review of such models is given in [20]. In this paper, we shall rely on equivalent circuit (EC) modelling of PE energy harvesters combined with the power conversion circuit and the electrical load. This approach is similar to that described in [21]. The model is based on the Butterworth-Van Dyke EC of a single PE element, but can be easily generalized to incorporate the more complex results from the finite-element analysis [20]. Since the EC model is kept simple, the freeware SPICE (Simulation Program with Integrated Circuit Emphasis) simulator of electronic circuits LTspice (Linear Technology Corporation, Milpitas, CA, USA) can be employed.

In order to be specific, the commercially available PE vibration energy harvester Mide$^{\text{TM}}$ PPA-1022 (Mide Technology Corporation, Medford, OR, USA) is used through the entire work [22]. It is a unimorph cantilever, where a single active PE layer (made of the PZT-5H material) is sandwiched between conductive and glass-reinforced epoxy laminate sheets [22]. By attaching an additional tip mass, the electromechanical resonance frequency of the circuit can be shifted below the resonance frequency of the free beam (nominal value is 408.4 Hz, $m_{\text{tip}} = 0$ g). The lumped model of a single PEC is shown in Figure 1 with the parameters of the linear EC model, tuned to the experimental resonance frequency of 40 Hz.
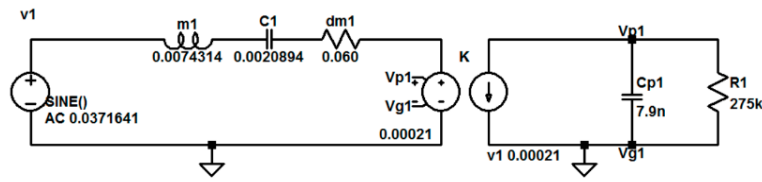
Figure 1. The lumped parameter model of a single piezoelectric cantilever (PEC) drawn in LTspice.

Figure 2 compares the simulated (denoted as "sim") and measured (denoted as "meas") results for the electrical power dissipated in the load resistance of 275 kΩ dependent upon the mechanical frequency f at a peak acceleration of 0.5 g_n, where g_n is the standard gravity. A softening-spring behavior is observed. Obviously, the conventional simulation ("con sim") cannot completely describe the nonlinear behavior of the PEC beam circuit. The behavior is reproduced very well only in the vicinity of the resonance frequency. When simulating an array with several beams, this nonlinear asymmetry effect is known to introduce some deviations between measurements and simulations [23]. We propose a simple adjustment to the common equivalent circuit for obtaining better simulation results of the entire array. From the recorded curve the bandwidth limits (half-power frequencies) f_1 and f_2 have to be determined. These frequency points are defined by the value of half of the maximum power, which can be extracted with the optimum resistance load. To match the common simulation, a new resonance frequency f_0' has to be calculated and the curve is shown in Figure 2 ("adj sim"). This new frequency is the geometric mean value of f_1 and f_2:

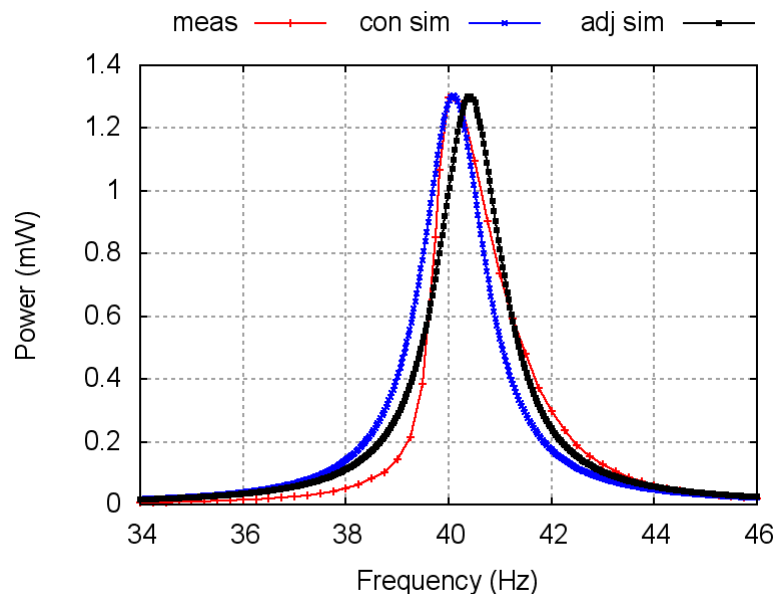$$f_0' = \sqrt{f_1 f_2} \tag{1}$$

Figure 2. Simulation (sim) of the conventional (con) and adjusted (adj) lumped element model compared to the measurements (meas).

Figure 2 shows that the resonance frequency of the adjusted simulation is slightly larger, but the half-power frequencies are reproduced correctly. This improvement leads to a much better similarity between the experimental and simulation results over a wider frequency band. The proposed correction changes to the EC parameters are small. The parameter adjustment works well since the quality factor of the resonance circuit is large ($Q \approx 25$). In the following, the lowest frequency limit of the array is determined by the lowest resonance frequency of a single (first) element, $f_0 = 40$ Hz ($m_{tip} = 7.4$ g).

The corresponding adjusted f_0' is equal to 40.39 Hz for the PEC used. The "adj sim"-curve corresponds to the parameters of the circuit shown in Figure 1.

Table 1 summarizes the parameters of the effective circuit model, tuned to the resonance frequency of 40 Hz. These parameters are the basis for the simulation of the entire PEC array. The notation corresponds to that shown in Figure 1.

Table 1. Nominal parameters of the equivalent circuit for the piezoelectric cantilever (PEC) tuned to the resonance frequency of 40 Hz.

Parameter	Abbreviation	Value
Effective mass	m1	7.58 mH
Stiffness (primary side)	C1	2.0894 mF
Damping resistance	dm1	0.060 Ω
Parallel capacitance	Cp1	7.9 nF
Electromechanical coupling	α	0.00021 As/m
Amplitude of excitation voltage	F_{AC}	0.0372 V

For mass tuning, the stiffness of the cantilever beam remains the same and only the effective mass must be changed. Therefore, the inductance on the primary side of the transformer (or, equivalently, the effective mass) must be adjusted in the equivalent circuit. If the new resonance frequency f_0' is determined from Equation (1), the corrected inductance can be easily calculated with the following formula: $m1' = m1 \times (f_0/f_0')^2$. For example, the adjusted effective mass in Figure 1 is related to the nominal effective mass of Table 1 as $(40/40.39)^2$.

As explained by the authors of [24–26], the common equivalent circuit model, consisting of an RLC circuit, can be constructed by the simplification of the cantilever beam to the mass-spring-damper system. An RLC circuit denotes an electrical circuit consisting of a resistor (R), an inductor (L), and a capacitor (C) (see Figure 1). The details can be found elsewhere in [20,21,24–26]. In the following we briefly outline the procedure of determining the effective parameters of the equivalent circuit. The parallel capacitance was measured directly using the RCL meter Hioki IM3533-01 (Hioki E.E. Corporation, Nagano, Japan). The effective mass was determined by the precision scales (Kern PCB350, Kern & Sohn GmbH, Balingen, Germany). In Table 1 the numerical value of inductance in H corresponds to the numerical value in kg. The spring constant (stiffness) was calculated from the resonance frequency. The damping resistance was derived from the decay constant of the impulse response of the output voltage. The electromechanical coupling coefficient was determined from the series and parallel resonance frequencies of the PEC electrical impedance [2] measured with an impedance spectroscope (HF2IS, Zurich Instruments, Zürich, Switzerland).

In the following theoretical considerations, it is assumed that all parameters of the equivalent circuit remain constant, except for the effective mass and the amplitude of the excitation voltage (excitation force), which is proportional to the effective mass. It will be seen below that such an approximation is reasonable in the present case.

The experiments were performed using the laboratory setup shown in Figure 3. The mechanical set up is mounted onto an electrodynamic shaker (Bruel & Kjaer Type 4826, Brüel & Kjaer Sound & Vibration, Nærum, Denmark), driven by a power amplifier (Bruel & Kjaer 2721). The signal for exciting the shaker is supplied by a waveform generator (Rigol DG4062, Rigol Technologies EU GmbH, Puchheim, Germany). The PEC array is mounted with the rigid metal frame onto the shaker (base plate); the clamping of the PECs (mechanical fixation) is done according to the specifications of the manufacturer. The tuning is achieved by weights fixed on the tips of the PECs. For a rough adjustment of a tip mass, the metal screw was employed while a modeling clay material was used for the fine tuning of the tip mass. The acceleration sensor serves to control the given value of acceleration amplitude.
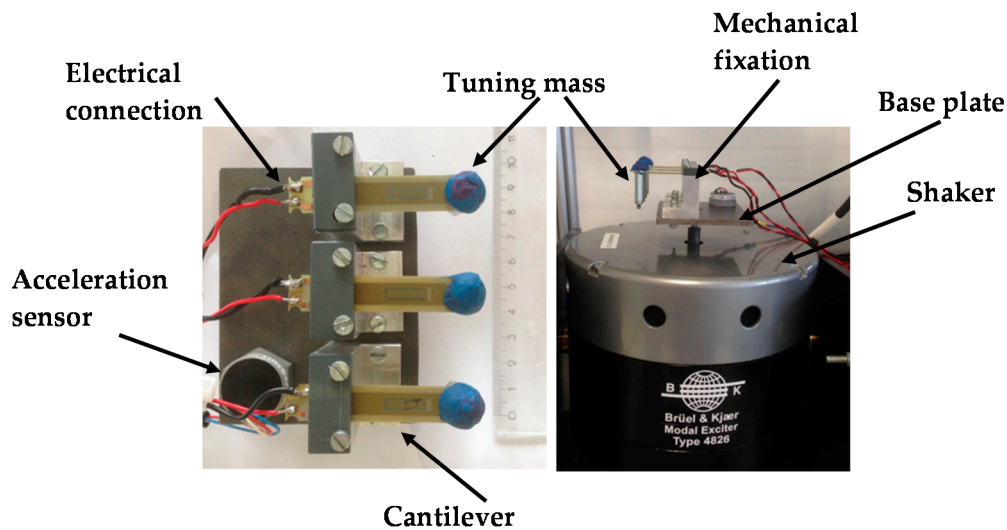
Figure 3. Mechanical set up with a PEC array.

3. Results and Discussion

First, we simulate the frequency dependence of the maximum output power from the PEC array. In Sections 3.1 and 3.2 the maximum electrical power deliverable by a PEC array is investigated theoretically. This means that each PEC is loaded by the resistance $R_L = 275$ kΩ and the power dissipated in each of these resistors is added. The electrical power determined in such a way represents the upper limit of the electrical power deliverable by such an array. In the real applications, the array should work on a single load. Therefore, in Section 3.3 we experimentally investigate connected PECs with individual full wave bridge rectifiers loaded by single resistance. Although the qualitative behavior of the bandwidth and the guaranteed electrical power with respect to the frequency detuning Δf between individual PECs remains the same as in the idealized case (Sections 3.1 and 3.2), there are some quantitative differences observed.

3.1. Optimum Detuning between Individual PE Cantilevers

Frequency tuning of a PEC can be done either by changing the effective mass or the beam stiffness. This can be achieved by variation of the cantilever geometry or material properties. In practical applications, commercially available PECs are likely to be resorted to. Such PECs are usually available in predefined steps of beam stiffness. Therefore, tuning by the tip mass is preferable. At upper frequencies the improvement by adding a further element with the higher resonance frequency to the array diminishes. As an example, Figure 4 shows that the peak power of the PEC 3 ($f_0 = 41.8$ Hz, $m_{tip} = 6.76$ g) is lower than the peak power of the PEC 1 ($f_0 = 40$ Hz, $m_{tip} = 7.4$ g) and PEC 2 ($f_0 = 40.9$ Hz, $m_{tip} = 7.07$ g). The reason for this behavior is the smaller beam deflection with the reduced tip mass.

Figure 5 presents simulated results for arrays with 2, 3, 4, and 5 PECs, where the detuning Δf is varied. The frequency bandwidth B (Figure 5a) is defined as the difference between the upper and lower frequencies, where the half of the peak electrical power harvested from the entire PEC array is reached. For a given number of array elements, an abrupt decrease of B (i.e., the steps seen in the plot) with the increasing detuning Δf is explained by the formation of a deep gap in the frequency dependence of the total electrical power P in the frequency region between the PEC with the highest resonance frequency and the PEC with the nearest lower resonance frequency (cf. Figure 6). As an example in Figure 6 shows, if the detuning Δf is too large, the resulting bandwidth is determined by two of three PECs. The curve "SUM" represents the sum of electrical powers in all three PECs.

Figure 5b displays the guaranteed power, which can be harvested from the array at a given value of Δf. From the results of Figure 5 the following conclusions can be drawn:

- The larger the frequency gap between the single PECs, the larger the bandwidth of the PEC array. This improvement works up to the certain maximum detuning Δf_{max}.
- The larger the frequency gap, the smaller the peak power. With the increasing detuning Δf, the peak power drops drastically and approaches a value which is practically independent of the number of PECs in the array.
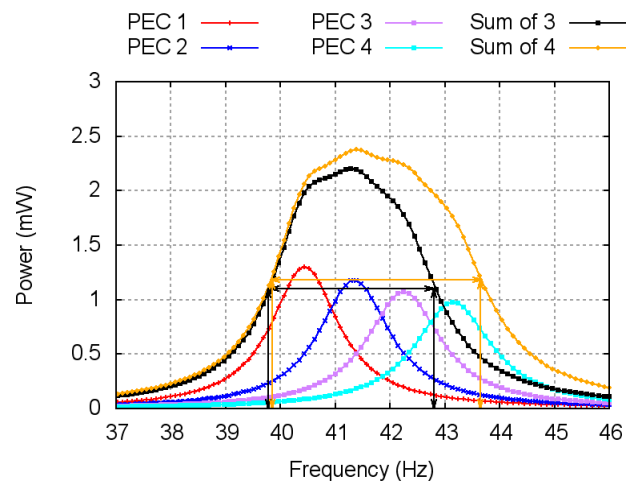
Figure 4. Simulated resonance curves of piezoelectric cantilever beam arrays.
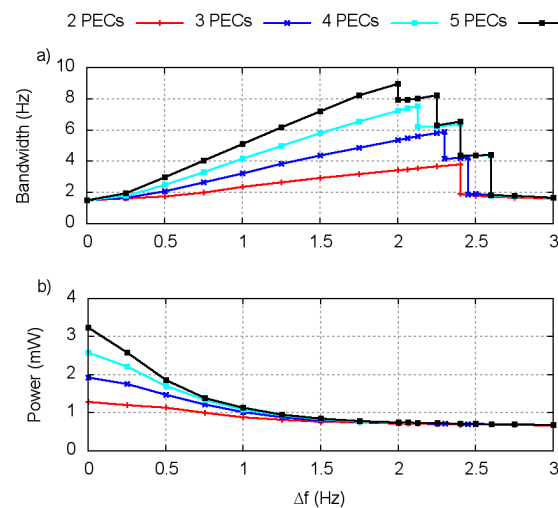
Figure 5. (**a**) Simulated dependence of the bandwidth on the frequency detuning Δf; (**b**) Dependence of the power at the half-power frequencies on the frequency detuning Δf.

To the best of our knowledge, the analysis presented in Figure 5 has been performed for the first time.
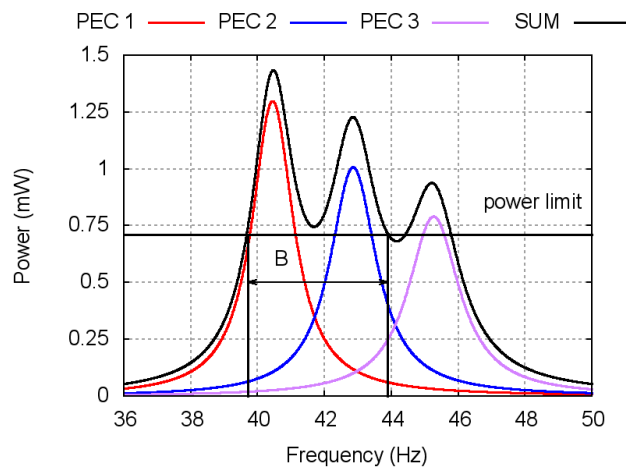
Figure 6. Simulated bandwidth of the array with large detuning Δf = 2.4 Hz.

3.2. Investigation of the Theoretical Maximum Bandwidth

3.2.1. Equidistant Gap Δf

In the preceding subsection, Figure 5 only showed the simulation of bandwidth up to a maximum of five cantilevers. However, it is possible to further increase the number of cantilevers and thus to increase the bandwidth. Figure 7 shows the theoretical maximum power of 12 cantilevers with Δf of 1.5 Hz and f_0 of the first PEC equal to 40 Hz. It is shown that the last cantilevers do not significantly increase the bandwidth. The reason for this behavior is the smaller amplitude of the last PECs due the smaller beam deflection with the reduced tip mass. Figure 8 shows the increase in bandwidth dependence on the number of cantilevers. It can be seen that beginning from 10 cantilevers, the bandwidth does not significantly increase. Therefore, an efficient number of cantilevers can be estimated as 10 with a maximum bandwidth of 13 Hz.
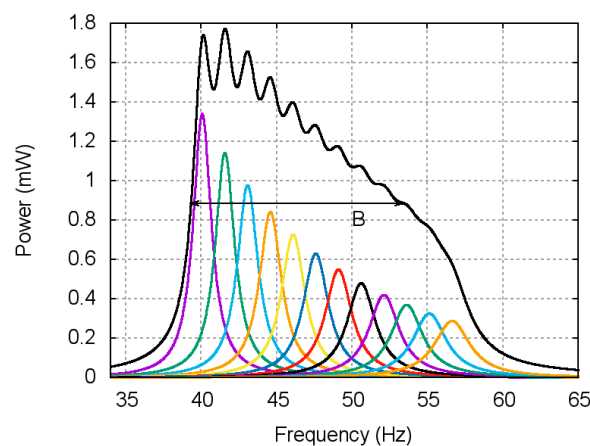

Figure 7. Simulation of a cantilever beam array with 12 cantilevers and Δf = 1.5 Hz.

The above observation can be made for various Δf. Figure 9a shows the dependence of the "effective" number of cantilevers (this means that the bandwidth does not significantly increase with an additional cantilever) on Δf. It can be seen that if Δf is decreasing, more cantilevers can be used, but the total bandwidth (see Figure 9b) improves only slowly. A further interesting aspect is that, although the number of cantilevers is increased and Δf is reduced, the bandwidth does not exceed a value of about 15 Hz. This means that the mass tuning is rather limited and a wide frequency spectrum cannot be achieved by mass tuning alone.
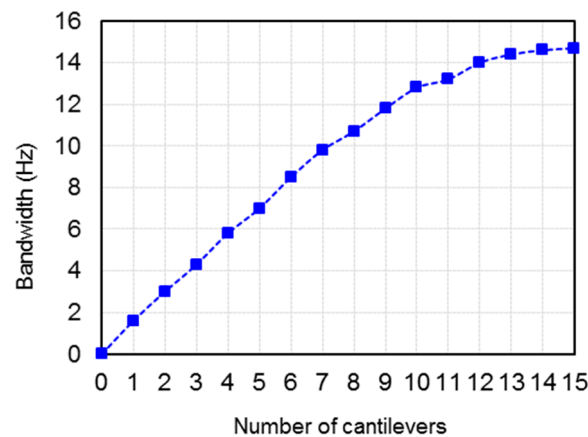
Figure 8. Simulation of bandwidth dependence on the number of cantilevers for $\Delta f = 1.5$ Hz. The lines connecting theoretical points serve as a guide for the eye.
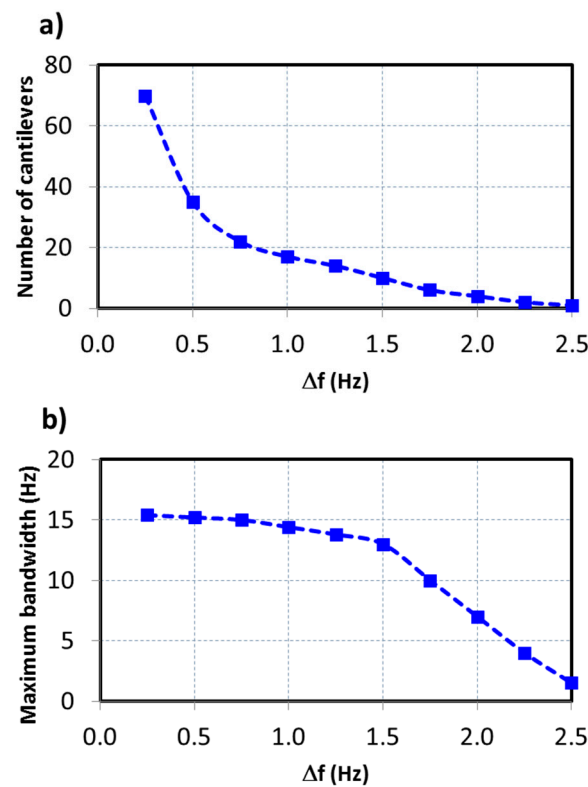

Figure 9. (**a**) Simulated dependence of the number of cantilevers on the frequency detuning Δf; (**b**) Dependence of the maximum bandwidth on the frequency detuning Δf. The lines connecting theoretical points serve as a guide for the eye.

3.2.2. Non-Equidistant Gaps Δf_i

In the previous section, different bandwidths with equidistant gaps of the resonant frequencies were analyzed. In the present subsection, the gaps between the resonant frequencies are not equidistant. All possible combinations of frequency gaps with 2, 3 and 4 cantilevers have been simulated with the resolution of 0.01 Hz. The combinations with the maximum theoretical bandwidth are shown in Table 2. The individual frequencies of the cantilevers do not vary significantly when increasing the number of cantilevers. This behavior is advantageous in the calculations of the optimum arrangements

of more cantilevers, because the simulation of all possible combinations of more than four cantilevers is time consuming. By using already identified frequencies for the simulation of a larger number of cantilevers, the computational complexity has been significantly reduced.

Table 2. The best theoretical arrangement to achieve the maximum theoretical bandwidth.

Number of cantilevers	Cantilever 1	Cantilever 2	Cantilever 3	Cantilever 4
2	40 Hz	42.4 Hz	-	-
3	40 Hz	42.4 Hz	44.64 Hz	-
4	40 Hz	42.4 Hz	44.7 Hz	46.7 Hz

Table 3 compares the theoretical maximum bandwidth for non-equidistant and equidistant gaps. The frequency bandwidth is larger for non-equidistant frequency detuning. However, the difference to the equidistant case is small. The reason for this is that, for a small number of cantilevers, the optimum frequency gaps of non-equidistant and equidistant cases are very similar. The advantage of non-equidistant frequency gaps over equidistant gaps increases with the growing total number of PECs.

Table 3. Comparison between the theoretical maximum bandwidth with non-equidistant and equidistant gaps between the resonant frequencies.

Non-Equidistant Gaps				
Number of Cantilevers	*Frequency Gaps*			*Maximum Bandwidth*
2	2.32 Hz	-	-	3.7 Hz
3	2.40 Hz	2.24 Hz	-	5.92 Hz
4	2.40 Hz	2.3 Hz	2.0 Hz	7.85 Hz
Equidistant Gaps				
Number of Cantilevers	*Frequency Gaps*			*Maximum Bandwidth*
2	2.32 Hz	-	-	3.7 Hz
3	2.25 Hz	2.25 Hz	-	5.7 Hz
4	2.1 Hz	2.1 Hz	2.1 Hz	7.4 Hz

3.3. Comparison with Experiment

The experiments were performed with nominally identical PECs as described above and shown in Figure 3. The resonance frequency was changed by fine adjustment of the tip mass. The parameters of the corresponding equivalent circuit are given in the Table 1, where only the effective mass and the amplitude of the excitation voltage must be modified accordingly. It is known that the effective mass of the cantilever beam can be calculated as m1 $= m_{tip} + (33/140)m_b$, where m_b is the beam mass [27]. In all experiments, the cantilever with the lowest resonance frequency of 40 Hz (PEC 1) is maintained constant.

In Sections 3.1, 3.2.1 and 3.2.2, all theoretical considerations were investigated for the case when each PEC is loaded by the experimentally obtained optimum resistance R_L = 275 kΩ. However, the replication of this optimum power in the experiment represents a challenge, when only the single load resistance is present. Many of the previous works investigated different approaches to connect individual cantilevers like parallel connection, series connection, connection with the full wave bridge rectifier, and SSHI or commercial LTC 3588 circuits. Most of the earlier works were based on the limitation that the cantilevers have the same resonance frequency and thus equal output voltage amplitude and phase. In the present work, the characteristics and limits of mass tuning are investigated from the perspective of the bandwidth enhancement. A striking feature of mass tuning is dependence of the voltage amplitude and phase on the adjustment mass. By usage of a single load, different voltage amplitudes have an impact on the previously investigated circuits. Figure 10 compares the series and

parallel connection of two cantilevers (PEC 1 and PEC 2 without rectifiers) with Δf of 1 Hz at the optimum resistance $R_{Lp} = R_L/2 = 137.5$ kΩ for parallel connection and $R_{LS} = 2R_L = 550$ kΩ for series connection with the optimum output power. The curves "PEC 1" and "PEC 2" show experimental dependences of both PECs loaded by the optimum resistance R_L without any rectifiers. The curve "PEC 1 + PEC 2" is the sum of dependences "PEC 1" and "PEC 2". It gives the experimentally obtained power limit (optimum power), which can be scavenged from these two energy harvesters. The curves "Simulation FB" and "Experiment FB" compare simulated and experimental dependences of the output power on the excitation frequency for these two PECs with respective electrical rectification (full bridge, FB) as shown in Figure 11.
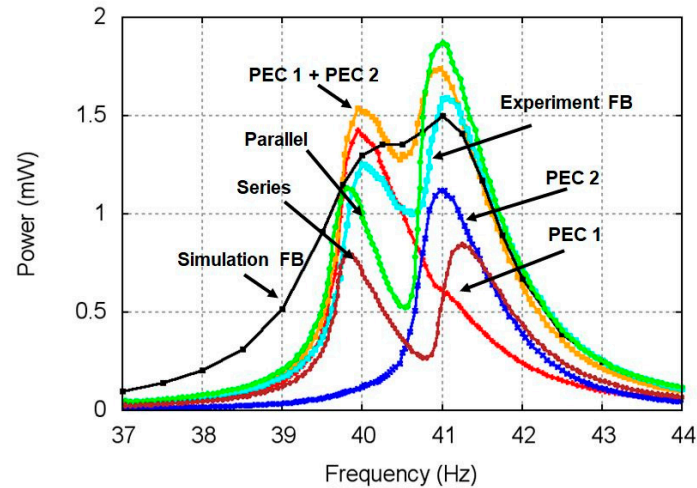

Figure 10. Power of parallel and series connection compared with the optimum power (designated as "PEC 1 + PEC 2"). FB: full bridge.
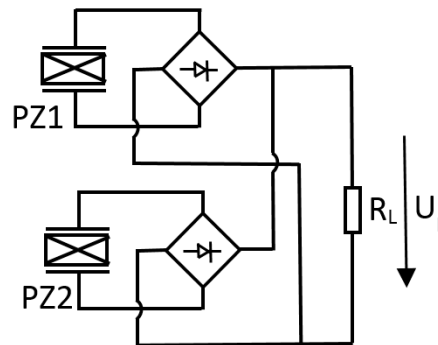

Figure 11. Two piezoelectric cantilevers (denoted as PZ1, PZ2) with the individual full wave bridge rectifiers connected parallel to the resistance R_L.

It can be seen in Figure 10 that, in some frequency regions, the resulting electric power of serial and parallel connections is much lower than the optimum power. The power loss is caused by different amplitudes and phases of the output voltage of two PECs. Without additional electrical components the maximum optimum power cannot be achieved with this setup in the broad frequency range. Figure 11 shows as an example a simple approach to scavenge the energy from two cantilevers close to the optimum value. This approach contains two standard FB rectifiers in parallel connection with the load R_L.

Figure 10 compares the optimum power of two harvesters (curve "PEC 1 + PEC 2") with the measurement of the parallel connection with two full wave bridge rectifiers and Δf of 1 Hz. It is seen that the measured power (curve "Experiment FB") is close to the optimum power. The observed

difference is caused by the power consumption of the diodes. Nevertheless, it is approximately possible to achieve the theoretical maximum power with a simple circuit.

However, the effectiveness of this circuit depends on the load resistance R_L. Figure 12 presents the dependence of the power dissipated the load resistance R_L for two PECs with Δf of 1 Hz at the excitation frequency of 40 Hz. The curve "PEC 1 + PEC 2" is the experimentally obtained power limit of the two separate PEC's without the full bridge rectifier. The curve "full bridge" shows the parallel connection with two full wave rectifiers in dependence on the load resistance. To facilitate the comparison, the electrical power is normalized to the total electrical power of two PECs individually loaded by the optimum resistance R_L = 275 kΩ. The interesting aspect is that the behavior of this circuit can be divided into three cases. At small load resistances (R_L < 75 kΩ) it is possible to scavenge more energy than the theoretical sum of two separate PEC's operating at the optimum load resistance of 275 kΩ. The reason for this behavior is the smaller internal resistance of the parallel connection. In the second case (75 kΩ < R_L < 220 kΩ), both PECs generate less electrical energy than the theoretical optimum. For large resistance loads (R_L > 220 kΩ), only one PEC with a higher voltage amplitude delivers the electrical energy to the load resistance. The reason is the higher output voltage of PEC 1 as compared to PEC 2. The higher output voltage blocks the diodes of the bridge rectifier of PEC 2 and only the diodes of PEC 1 are conductive.
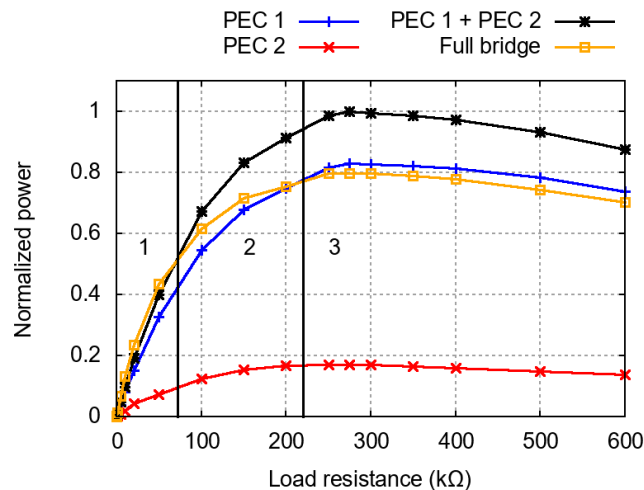

Figure 12. Dependence of the normalized electrical power on the load resistance.

To verify theoretical considerations, the dependence of achieved bandwidth on frequency detuning Δf was investigated experimentally. Figure 13 presents two cases, (a) and (b) with two cantilevers, and (c) and (d) with three cantilevers. There are three graphs compared in each figure. The first graph shows the simulated theoretical maximum bandwidth as described in Section 3.1, while the second graph represents the simulated parallel connection with rectifiers at its optimum resistance. The third curve demonstrates the measured results for the parallel connection with rectifiers at its optimum resistance. From the diagrams, it can be seen that the agreement between theoretical and experimental bandwidths at low frequency detuning (Δf < 1.7 Hz) is good. However, the simulated and experimentally observed "jumps" (cf. Section 3.1) of the bandwidth differ by approximately 0.2–0.5 Hz. The difference between the two simulated curves can be explained by diode losses.

Figure 13 also demonstrates the involvement of several harvesters in bandwidth widening and enhancement of the output power. If $\Delta f \to 3$ Hz, a single PEC determines the frequency bandwidth ($\approx$1.2 Hz) and the guaranteed output power of the array ($\approx$0.65 mW) within the working frequency range. Even a cantilever working farther away from its resonance frequency brings its contribution to the frequency bandwidth and the output power. Figure 13a,c show that there are frequency detuning regions where the frequency bandwidth can be increased by more than two or three times, respectively.

It is observed that in these frequency detuning regions, the total output power of the array can be significantly larger than the maximum guaranteed power of 0.65 mW from the single PEC.

To illustrate the difference between the measurement and the simulation, Figure 14 depicts two individual measuring points for two cantilevers. The first measurement point is Δf = 1.5 Hz, where there is reasonable agreement between the simulation and the experiment. The second measuring point at Δf = 2 Hz is where the differences are easily noticeable. Figure 15 presents the differences for the case of three PECs.
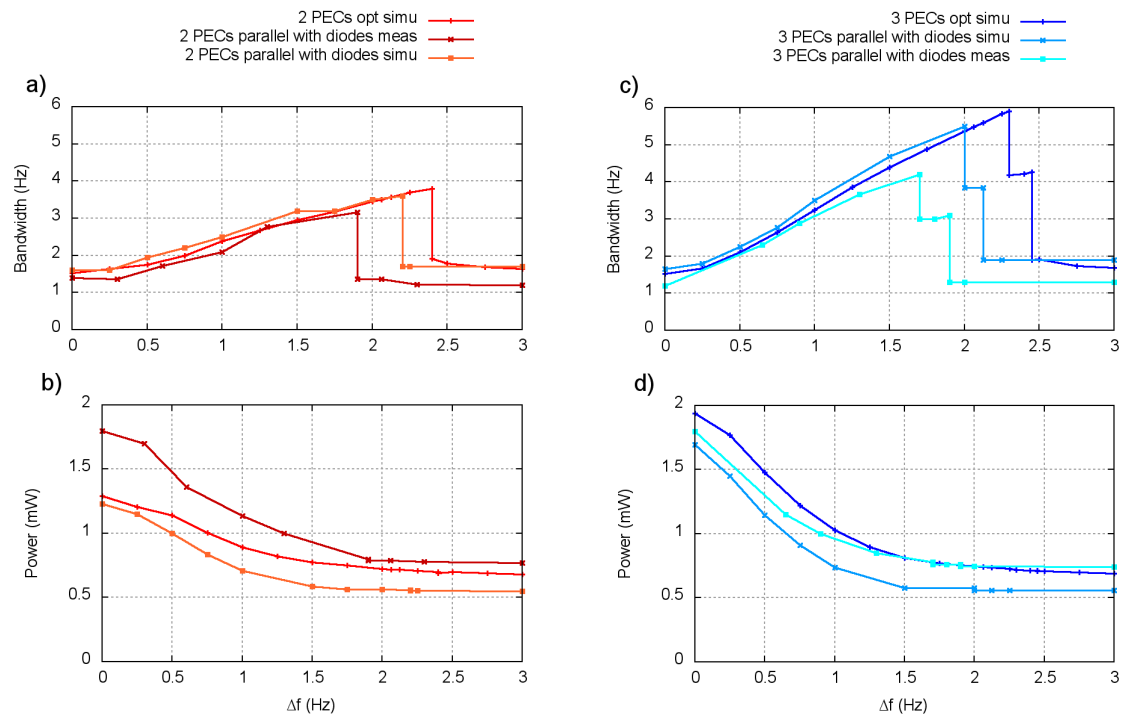

Figure 13. Comparison of the frequency dependency of the bandwidth (**a**,**c**) and the guaranteed electrical power (**b**,**d**) between simulation and measurement for arrays with two (**a**,**b**) and three (**c**,**d**) PECs.
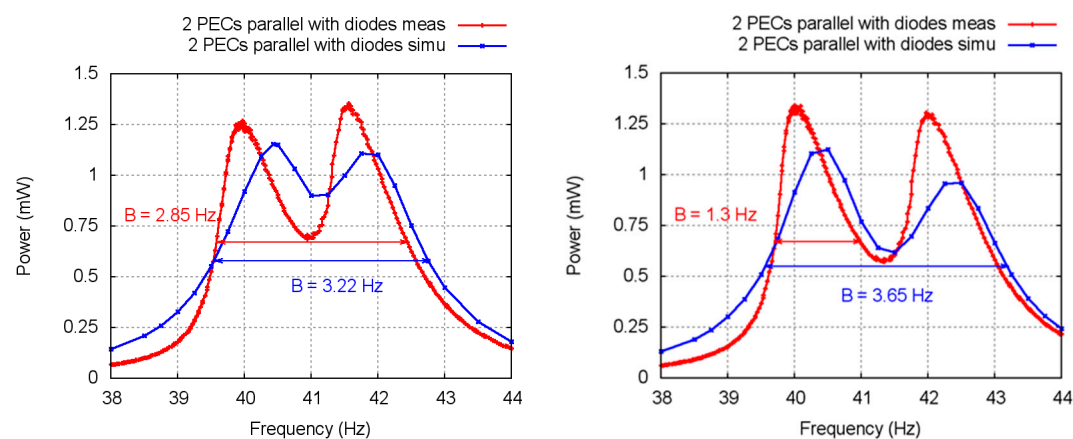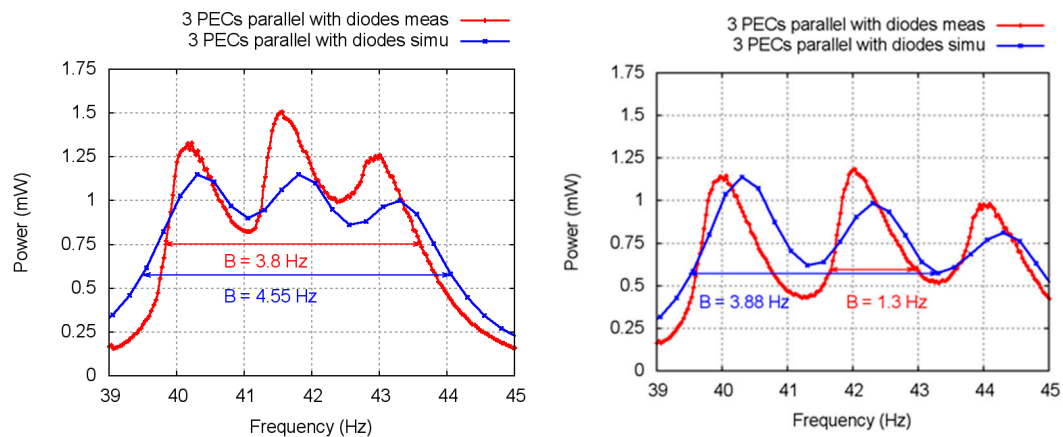

Figure 14. Comparison of the simulated and measured power with dependence upon frequency for the parallel connection of two PECs with individual rectifiers and Δf = 1.5 Hz (**left**) or Δf = 2 Hz (**right**).

Figure 15. Comparison of the simulated and measured power with dependence upon frequency for the parallel connection of three PECs with individual rectifiers and Δf = 1.5 Hz (**left**) or Δf = 2 Hz (**right**).

As explained in [19], the disadvantage of a PEC array design with frequency-detuned cantilevers based on the overall electrical rectification is the inevitable charge cancellation causing lower power output. In the present paper, we considered the respective electrical rectification of individual PEC outputs. In the considered experimental situation, such an approach seems to pay off with respect to the achieved frequency bandwidth and guaranteed output power. Obviously, the complexity of the electronic circuitry is somewhat increased in comparison to the overall electrical rectification due to the presence of additional rectifiers.

The discrepancies between the simulation results and the experiments are obviously explained by the imperfection of the model. One reason for these differences is the non-linear behavior of cantilevers. The resonance curve is noticeably asymmetric with respect to the resonance frequency, which can be attributed to the softening behavior of the cantilever [28]. Although the bandwidth can be reproduced sufficiently well with the simplifying approach of Section 2, the course of frequency dependencies between the half-power-frequencies for measurements and simulations is different. Therefore, the nonlinearity of the cantilevers should be considered in the future simulations, in order to achieve better agreement. Furthermore, some differences can be seen in the voltage amplitudes of the individual PECs. We attribute these differences to the additional mechanical coupling the cantilevers through the base plate where they are fixed. The model should be extended to include the coupling through the base plate into the simulations in order to achieve a better accuracy. However, it is observed that even a simplified model such as that presented in this paper is useful since it provides reasonable agreement with experiments and allows one to understand the basic regularities of vibration energy harvesting with tip-mass tuned PECs. We believe that general conclusions derived in this paper (in particular, in Section 3.2) are generally valid. However, there may be refinements necessary as far as alternative realizations of PECs are concerned. In particular, it would be interesting to investigate how the damping factor and the effective constants of different PEC realizations may change as the magnitude of the tip mass increases and what the implications are on the achieved frequency bandwidth.

4. Conclusions

This paper provides practical guidelines for optimum design of PEC beam arrays employed for low-frequency vibration energy harvesting. The useful bandwidth can be extended by increasing the number of piezoelectric cantilevers distributed over the desired frequency band. Frequency tuning of a piezoelectric cantilever can be done by changing the effective mass. However, tip-mass tuning is limited and the achievable bandwidth reaches saturation for the increasing number of PECs. For a small number of PECs, realization of non-equidistant resonance frequency gaps seems to bring little

advantage in comparison to equidistant resonance frequency gaps. The output voltages of individual PECs at a particular excitation frequency have different amplitudes and phases, because the resonance frequency of each PEC is different. It is shown that a simple power-transfer circuit where several PECs with the individual full wave bridge rectifier are connected in parallel allows one to extract the electrical power close to the theoretical maximum excluding the diode losses. The experiments made on two- and three-PEC arrays are in accordance with simulations and show that this power-transfer circuit additionally influences the frequency dependence of the harvested electrical power.

Author Contributions: M.S. conceived and designed the experiments; E.D. and F.F. performed the experiments; E.D., L.Y.F. and M.S. analyzed the data; E.D. developed the model and performed the simulations; E.D. and M.S. wrote the paper. All authors reviewed the manuscript.

Conflicts of Interest: The authors declare no conflict of interest.

References

1. Bogue, R. Energy harvesting and wireless sensors: A review of recent developments. *Sens. Rev.* **2009**, *29*, 194–199. [CrossRef]
2. Priya, S.; Inman, D. *Energy Harvesting Technologies*; Springer: New York, NY, USA, 2009.
3. Erturk, A.; Inman, D. *Piezoelectric Energy Harvesting*; Wiley: Chichester, UK, 2011.
4. Briand, D.; Yeatman, E.; Roundy, S. (Eds.) *Micro Energy Harvesting*; Wiley-VCH Verlag: Weinheim, Germany, 2015.
5. Tang, L.; Yang, Y.; Soh, K. Toward broadband vibration-based energy harvesting. *J. Intell. Mater. Syst. Struct.* **2010**, *21*, 1867–1895. [CrossRef]
6. Twiefel, J.; Westermann, H. Survey on broadband techniques for vibration energy harvesting. *J. Intell. Mater. Syst. Struct.* **2013**, *24*, 1291–1302. [CrossRef]
7. Shahruz, M. Design of mechanical band-pass filters for energy scavenging. *J. Sound Vib.* **2006**, *292*, 987–998. [CrossRef]
8. Shahruz, M. Limits of performance of mechanical band-pass filters used in energy scavenging. *J. Sound Vib.* **2006**, *293*, 449–461. [CrossRef]
9. Xue, H.; Hu, Y.; Wang, Q.M. Broadband piezoelectric energy harvesting devices using multiple bimorphs with different operating frequencies. *IEEE Trans. Ultrason. Ferroelectr. Freq. Control* **2008**, *55*, 2104–2108. [PubMed]
10. Ferrari, M.; Ferrari, V.; Guizzetti, M.; Marioli, D.; Taroni, A. Piezoelectric multifrequency converter for power harvestinrg in autonomous microsystems. *Sens. Actuators A Phys.* **2008**, *142*, 329–335. [CrossRef]
11. Liu, H.; Tay, C.; Quan, C.; Kobayashi, T.; Lee, C. Piezoelectric MEMS energy harvester for low-frequency vibrations with wideband operation range and steadily increased output power. *J. Microelectromech. Syst.* **2011**, *20*, 1131–1142. [CrossRef]
12. Al-Ashtari, W.; Hunstig, M.; Hemsel, T.; Sextro, W. Enhanced energy harvesting using multiple piezoelectric elements: Theory and experiments. *Sens. Actuators A Phys.* **2013**, *200*, 138–146. [CrossRef]
13. Wen, Z.; Deng, L.; Zhao, X.; Shang, Z.; Yuan, C.; She, Y. Improving voltage output with PZT beam array for MEMS-based vibration energy harvester: Theory and experiment. *Microsyst. Technol.* **2015**, *21*, 331–339. [CrossRef]
14. Zhao, X.; Shang, Z.; Luo, G.; Deng, L. A vibration energy harvester using AlN piezoelectric cantilever array. *Microelectron. Eng.* **2015**, *142*, 47–51. [CrossRef]
15. Wu, P.H.; Chen, Y.J.; Li, B.Y.; Shu, Y.C. Wideband energy harvesting based on mixed connection of piezoelectric oscillators. *Smart Mater. Struct.* **2017**, *26*, 094005. [CrossRef]
16. Lumentut, M.F.; Francis, L.A.; Howard, I.M. Analytical techniques for broadband multielectromechanical piezoelectric bimorph beams with multifrequency power harvesting. *IEEE Trans. Ultrason. Ferroelectr. Freq. Control* **2012**, *59*, 2555–2568. [CrossRef] [PubMed]

17. Lien, I.C.; Shu, Y.C. Array of piezoelectric energy harvesting by the equivalent impedance approach. *Smart Mater. Struct.* **2012**, *21*, 082001. [CrossRef]

18. Lin, H.C.; Wu, P.H.; Lien, I.C.; Shu, Y.C. Analysis of an array of piezoelectric energy harvesters connected in series. *Smart Mater. Struct.* **2013**, *22*, 094026. [CrossRef]

19. Lien, I.C.; Shu, Y.C. Piezoelectric array of oscillators with respective electrical rectification. *Proc. SPIE* **2013**, *8688*, 868806.

20. Yang, Y.; Tang, L. Equivalent circuit modelling of piezoelectric energy harvesters. *J. Intel. Mater. Syst. Struct.* **2009**, *20*, 2223–2235. [CrossRef]

21. Romani, A.; Paganelli, R.; Sangiorge, E.; Tartagni, M. Joint modeling of piezoelectric transducers and power conversion circuits for energy harvesting applications. *IEEE Sens. J.* **2013**, *13*, 916–925. [CrossRef]

22. PPA Products Data Sheet—User Manual. Available online: https://info.mide.com/piezo-products/download-piezo-products-datasheets (accessed on 6 December 2017).

23. Lee, S.; Kang, D.; Je, Y.; Moon, W. Resonant frequency variations in a piezoelectric microcantilever sensor under varying operational conditions. *J. Micromech. Microeng.* **2012**, *22*, 105035. [CrossRef]

24. Al-Ashtari, W.; Hunstig, M.; Hemsel, T.; Sextro, W. Analytical determination of characteristic frequencies and equivalent circuit parameters of a piezoelectric bimorph. *J. Intel. Mater. Syst. Struct.* **2012**, *23*, 15–23. [CrossRef]

25. Shu, Y.C.; Lien, I.C. Efficiency of energy conversion for a piezoelectric power harvesting system. *J. Micromech. Microeng.* **2006**, *16*, 2429. [CrossRef]

26. Zhou, L.; Sun, J.; Zheng, X.J.; Deng, S.F.; Zhao, J.H.; Peng, S.T.; Zhang, Y.; Wang, X.Y.; Cheng, H.B. A model for the energy harvesting performance of shear mode piezoelectric cantilever. *Sens. Actuators A Phys.* **2012**, *179*, 185–192. [CrossRef]

27. Knaebel, M.; Jäger, H.; Mastel, R. *Technische Schwingungslehre*; Springer: Wiesbaden, Germany, 2009. (In German)

28. Nguyen, D.S.; Halvorsen, E. Analysis of vibration energy harvesters utilizing a variety of nonlinear springs. *Proc. Power-MEMS* **2010**, *10*, 331–334.